Prediction of annular flows in vertical pipes with new correlations for the CATHARE-3 three-field model

M. Spirzewski, P. Fillion, M. Valette

PREDICTION OF ANNULAR FLOWS IN VERTICAL PIPES WITH NEW CORRELATIONS FOR THE CATHARE-3 THREE-FIELD MODEL

Michał Spirzewski,
NCBJ
UZ3, 05400 Otwock, Poland
michal.spirzewski@ncbj.gov.pl

Philippe Fillion
CEA, DEN-Service de Thermohydraulique et de Mécanique des Fluides, STMF, Université Paris-Saclay
F-91191 Gif-sur-Yvette, France
philippe.fillion@cea.fr

and Michel Valette
CEA, DEN-Service de Thermohydraulique et de Mécanique des Fluides, STMF
F-38054 Grenoble, France
michel.valette@cea.fr

ABSTRACT

Prediction of the critical heat flux is crucial for boiling system such as water cooled reactors. In the case of high steam qualities in the core, occurrence of the critical heat flux, also called dryout, is usually associated with evaporation of thin liquid film from the heated rods, thus leaving their clad in direct contact with the vapor phase. Several phenomena – annular flow transition with corresponding initial conditions as well as entrainment and deposition of the droplets from or onto the liquid film – require appropriate modeling in order to accurately estimate the occurrence of the dryout and its location.

This work re-evaluates the models of CATHARE-3 system code with the extended data base of adiabatic and diabatic tests in vertical pipes. At the same time, a comparative study is performed which aims at the validation of the alternative model for entrainment and deposition of the droplets for the three-field model of the CATHARE-3 code. On one hand, extended adiabatic database shows area where the new models improve the prediction as well as indicates what the common weaknesses of both models are. On the other hand, extended diabatic database shows that current models of boiling entrainment and deposition inhibition for high pressures overpredict measured values for experiments with high heat fluxes. Moreover, the inherent models of CATHARE-3 are extended by the implementation of the Initial Entrainment Fraction (IEF) phenomenon. The model for IEF is developed using KTH film flow experiment and validated with diabatic Wurtz experiments. New set of models improve the predictions of droplet field against this database.

KEYWORDS
dryout, annular flow, CATHARE, three-field model

1. INTRODUCTION

All light water nuclear reactors' designs are limited by the critical heat flux phenomenon as far as the power production is concerned. The CHF depends on many different mechanisms and flow conditions and its evaluation is complex and not straightforward. Regardless of the mechanisms involved, the CHF for the high quality flows (which can be classified as “dryout”) is usually defined as the sudden rise of the temperature of the heating element - a fuel rod in light water reactor systems. The aforementioned rise occurs when the thin water film is evaporated from the surface of the rod which causes exposure of that surface to the vapor phase.

Despite the apparent definition of this phenomenon a lot of effort has been spent on proper modelling of involved mechanisms which would allow predicting the dryout limit. So far a lot of different empirical correlations have been utilized, which can be characterized with high accuracy and reliability for some specific geometries and flow conditions, but they lack the ability to capture the physics of the dryout.

Since dryout is a hydrodynamic phenomenon involving entrainment and deposition of the droplets as well as evaporation of the liquid, knowledge of all these mechanisms is required to quantitatively estimate the dryout location. Over past several decades large number of experimental and theoretical studies have been conducted in order to understand the underlying processes [1]. With these works, the empirical models have been changed into phenomenological models which enabled better predictions of dryout location using mass balance equations [2].

This paper presents the current status and approach of dryout modelling applied in CATHARE-3 system code with its results as well as the modification utilized in order to improve the results.

2. MODELS OF ENTRAINMENT AND DEPOSITION IN CATHARE-3

The three-field model of the CATHARE 3 system code is based on a nine-equation system, three mass balance equations, three momentum equations and three energy balance equation for each of the 3 fields: continuous liquid, liquid droplets and gas phase. This model has been previously described and assessed for vertical two-phase flows in tubes and rod bundles [3, 4]. In these papers, the validation matrix included experimental data for entrainment and deposition terms in adiabatic and diabatic conditions. A first set of closure laws for LBLOCA application (Large Break Loss of Coolant Accident) has also been assessed against reflooding separate effect tests (PERICLES and RBHT) and against the reflooding phase of such a postulated accident simulated on BETHSY facility [5].

Current version of CATHARE-3 three field model is comprised of annular flow criterion and entrainment and deposition phenomena which occur during annular flow. The criterion for annular flow regime is realized by fulfilling two conditions. The first condition is the Kutateladze number (see equation (8)) being higher than 3.2 and the second one is the void fraction being higher than 0.5. It must be pointed out that to satisfy smoothness of the transition a spline function is implemented for both conditions.

As far as entrainment and deposition phenomena are concerned, they can be divided into two groups: a non-boiling and boiling induced. The non-boiling entrainment (caused by shear stress induced by vapor on liquid film) and deposition (caused by turbulence in the gas core) phenomena are modeled by Hewitt-Govan correlations [6]:

$$m_{E,HG} = 5.75 \times 10^{-5} G_v \left[\left(G_{lf} - G_{lfc} \right)^2 \frac{D_h \rho_l}{\sigma {\rho_v}^2} \right]^{0.316} \quad (1)$$

$$m_{D,HG} = C \cdot 0.083 \left[\frac{\rho_v D_h}{\sigma} \right]^{-1/2} \max\left(0.3, \frac{C}{\rho_v} \right)^{-0.65} \quad (2)$$

where G is the mass flux, subscripts v, lf and lfc represent vapor, liquid film and critical liquid film respectively, and D_h is the hydraulic diameter. Additionally, G_{lfc} and C are defined as follows:

$$G_{lfc} = \frac{\mu_l}{D_h} \exp\left(5.8504 + 0.4249 \frac{\mu_v}{\mu_l} \sqrt{\frac{\rho_l}{\rho_v}} \right) \quad (3)$$

$$C = \frac{\alpha_d \rho_d}{\alpha_d + \alpha_v} = \frac{\alpha_d \rho_d}{1 - \alpha_f} \quad (4)$$

Two boiling phenomena are included in the considered flow regime. One contributes positively to the entrainment phenomenon. Specifically, liquid droplets that are “ripped off” of the liquid film by vapor bubble coming from heated wall with significant velocity. This phenomenon is modelled by the Ueda et al. correlation [7]:

$$m_{E,B} = C_{\text{fluid}} \left(\frac{q''}{h_{fg}} \right)^{2.5} \left(\frac{\delta_{\text{film}}}{\sigma \rho_v} \right)^{0.75} \quad (5)$$

where C_{fluid} is a constant dependent on the fluid (C_{fluid}=477 for water) and δ_{film} is the film thickness which can be approximated by $\delta_{\text{film}} = \alpha_l D_h / 4$.

However, this correlation was devised basing on data coming from the experiment conducted in roughly atmospheric pressure and thus its usage is debatable in high pressure conditions, such as those occurring in BWRs.

The second boiling phenomenon negatively influences the deposition - namely, the bubble escaping the film inhibits the deposition of liquid droplets on the liquid film. This phenomenon was correlated by Hoyer [8]:

$$\Gamma_d = \frac{4}{D_h} \rho_{ld} \frac{\alpha_{ld}}{\alpha_{ld} + \alpha_g} \max\left(k_D - k_q, 0 \right) \quad (6)$$

where k_D is the contribution to deposition due to turbulence, calculated by Hewitt-Govan correlation (equation (2)), while k_q is relative to a deposition inhibition to boiling effects and is calculated as:

$$k_{\text{q}} = \frac{\Gamma_{\text{lcv}}}{0.065 \rho_{\text{lc}}} \frac{D_{\text{h}}}{4\sqrt{\alpha_{\text{ld}} + \alpha_{\text{v}}}} \quad (7)$$

At the transition between churn-turbulent and annular flow, a rate of annular flow (from 0 to 1) is calculated and then taken into account in calculating the rate of entrainment which in a way sets the way the entrainment is initiated.

As mentioned at the beginning of this section, presented set of equations was tested on the extensive database which consisted of four adiabatic experiments and two experiments with heat transfer. The validation matrix included Becker, Bennett and Wurtz (see Table 1) [9] experiments in tube, and TPTF and THTF rod-bundle experiments. Despite the fact that overall simulation results fit (non-linear least squares fit is applied) decently with the experimental results, noticeable spread occurs in some of adiabatic cases. This can be exemplified in Figure 1a where the “current CATHARE-3” model is marked with red colour. Results obtained on high pressure databases, such has Wurtz series 200, show that Hewitt-Govan model tends to strongly underpredict the entrained flowrate for some runs. Further analysis indicates this underestimation occurs at low gas flowrates, behaviour also noticed by Okawa [11].

Similar behaviour of said set of equations is observed (in Wurtz series 300 diabatic experiment depicted in Figure 1b. However, when the case of much higher heat flux and qualities is concerned, the accuracy of this set of equations is questioned. Namely, KTH Film Flow experiment [11] in Figure 4 shows the film flow with respect to the axial position. Current state of mass balance equations in CATHARE-3 significantly underpredicts the amount of film in the simulation (which resulted in dryout, against experimental observations), which is directly translated as an overprediction of the droplet field. These sample results prove that more accurate modelling is necessary to predict the entrainment in adiabatic and diabatic conditions.

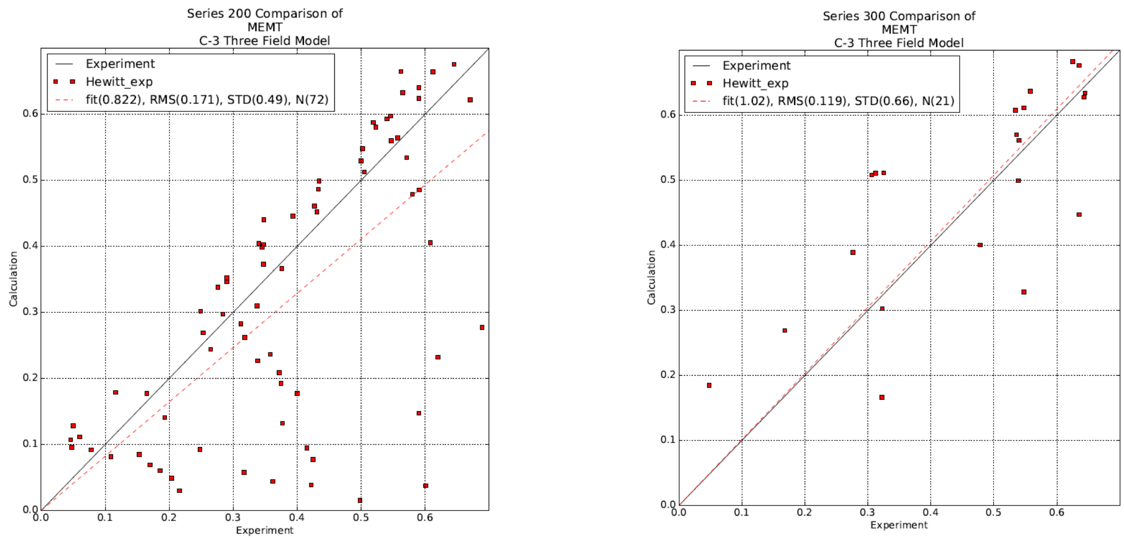

(a) (b)

Figure 1. Calculation results obtained with „current CATHARE-3 model" compared with: (a) Wurtz 200 Series adiabatic experiment (b) Wurtz 300 Series boiling experiment. M_e/M_t (denoted MeMt in the figures) is the ratio of the entrained (droplet) flowrate M_e to the total flowrate (liquid and vapor) M_t.

3. SELECTION OF NEW MODELS

An intensive literature study has been carried out, first to select models allowing to better predict the amount of droplets in adiabatic conditions, then to improve the description of the three fields under heating conditions, especially where the dryout may appear. The occurrence of dryout is dependent on many different phenomena and variables. The heat flux being the most influential because it drives the film evaporation. Other variables affect the estimation of dryout indirectly through the mass transfer between continuous and dispersed liquid phases. These are the length of the annular flow, conditions at the onset of the annular flow, entrainment and deposition mass transfer rates and finally, criterion for dryout. In this paper only the hydrodynamic processes are discussed – specifically: onset of annular flow, initial entrained fraction and entrainment and deposition mass transfer rates.

3.1 Onset of Annular Flow

As far as onset of annular flow is concerned, there are two major correlations which provide the information about the transition to annular flow, namely Kutateladze [12] and Wallis [13].
The first is defined as follows:

$$Ku = \alpha_v V_v \left(\frac{\rho_v^2}{g\sigma(\rho_l - \rho_v)} \right)^{1/4} \tag{8}$$

and is used in CATHARE-3 code with the critical value being 3.2. The latter is based on the dimensionless superficial velocity of phases defined as, for each phase *k*:

$$J_k^* = J_k \sqrt{\frac{\rho_k}{gD_h(\rho_l - \rho_v)}} \tag{9}$$

and several values around unity for the gas phase are recommended in the literature [1,13] as the transition to annular flow. Okawa in his publication [10] used value of 2 to make sure that annular flow is fully developed. Another approach for utilizing the Wallis criterion to predict the onset of annular flow is presented in [14] where the following correlation is incorporated:

$$J_v^* = 0.4 + 0.6 \cdot J_l^* \tag{10}$$

This criterion can be transformed into a so-called "transition quality" which is calculated as follows:

$$x_{tr} = \frac{0.6 + 0.4\sqrt{\rho_l(\rho_l - \rho_v)gD_h}\,/\,G}{0.6 + \sqrt{\rho_l/\rho_v}} \tag{11}$$

These two equations can be used interchangeably and this approach is used in the final modelling package.

3.2 Initial Entrainment Fraction

With the transition to the annular flow one of the crucial parameters of the flow is the distribution of liquid water between droplets and film. This boundary condition is usually called "Initial Entrainment Fraction" (IEF), where the entrainment fraction *E* corresponds to the ratio of the droplet flowrate to the total liquid (droplet + film) flowrate.

Throughout the literature this boundary condition is expressed either through mass fraction or volume fraction.

With the development of the different correlations for the entrainment and deposition, which will be discussed later in this paper, several approaches for IEF estimation are to find. The first approach bases on the two extreme cases of liquid water distribution, specifically, all water is either in the film field or in the droplet field [15, 2]. However, the authors of these publications were aware that such conditions were unrealistic but yielded reasonable results and postulate that calculations for the flow rates of liquid film and entrained droplets at the measurement point are insensitive to the selection of the initial condition.

The second approach postulates the equilibrium state of the flow conditions where both phenomena - entrainment and deposition - are equal. This approach was used by Govan [16] where homogeneous flow - initial void fraction of 50% - at the start of the annular flow was postulated. According to this author, location of dryout on experiments with uniform axial power shape is quite sensitive to the initial conditions, namely the droplet fraction, at the transition.

The extension of the previous approach is presented by Okawa in [10] and [14] where the initial entrainment fraction E_{init} is calculated from assumption of equality between entrainment and deposition correlation suggested by the author and thus:

$$E_{\text{init}} = \frac{E_{eq}}{1 - E_{eq}} = \frac{1}{4}\frac{k_E}{k_D}\frac{\sqrt{f_i f_w}\sqrt{\rho_v \rho_l}\,J_v^2 D_h}{\sigma}\left(\frac{\rho_l}{\rho_v}\right)^n \tag{12}$$

However, this approach is disproved by Barbosa et al. [17] in the experiment where the IEF is calculated for equilibrium conditions using Hewitt-Govan correlations. The authors show that with increasing mass flux the calculated values' deviation from the experimental measurements increases.

Only the most recent studies show attempts in proposing correlation derived from experimental measurements. Anglart [18] suggested a correlation for the *film* fraction which is based on Reynolds liquid number and Boiling number. The film fraction correlation is a part of "modelling package" which is supplemented with Wallis annular flow criterion and Hewitt-Govan models for entrainment and deposition phenomena. Presented results fit the experimental measurements well.

Another film fraction correlation is due to Oh et al., [19] which depends on the total Reynolds number developed from Wurtz database, representative of annular transition in BWR fuel bundles. The proposed correlation gives a reasonable agreement against these experiments, however, its validation was not showed on other experiments.
A bit more sophisticated approach is presented by Dasgupta [20], based on a triangular relationship between the film flowrate, film thickness and two-phase pressure drop. It is postulated that knowing any two of these quantities allows calculation of the third. The author suggests calculation of the pressure drop with two different formulas. One which considers the IEF, and one which is independent on such quantity. In his later paper [21] this method is supplemented with the criterion for distinguishing low and high values of IEF which were acquired through his method.

3.3 Non-boiling Phenomena

The entrainment-deposition phenomena consists of couple different mechanisms that contribute to the mass exchange between droplet and film field. First approaches to model this contribution based on lumping all mechanisms under one general correlation for each contributor. One of the most used correlations is one of the Hewitt-Govan mentioned previously in text which is based on the minimum (or critical) film flow, for entrainment, and droplet diffusion for deposition. Throughout the literature one can encounter various modification of this formula which aim to satisfy different geometrical nuances and pressures.
Similar lumped approach is utilized by Sugawara [15] which is then used in the in-house FIDAS code. His correlation for entrainment is based on a series of dimensionless parameters which take into account effects of density ratio, forces acting on the film and gas velocities which are then accordingly fit to the experimental data. As far as deposition correlation is concerned it is based on turbulent diffusivity of entrained droplets in the vapor core. The author correlates the experimental measurements with gas core Reynolds number and Schmidt number.
Interesting correlation which is more recent is the Okawa [10] formula which bases on that entrainment is caused by the breakup of roll wave due to interfacial shear force. In principle, it is similar to the Sugawara entrainment formula but the Okawa model is modelled slightly different. Okawa's assumption is expressed by the proportion of the interfacial shear force $f_i \rho_v J_v^2$ to the surface tension force σ/δ. This proportion is expressed by the dimensionless number π_E:

$$\pi_E = \frac{f_i \rho_v J_v^2 \delta}{\sigma} \tag{13}$$

This number is a basis for other variation of the entrainment correlation which is then analyzed in Okawa's following publications [14,22,23]. The variations of the Okawa model were not tested in this paper. Results obtained by Secondi et al. [26] showed a derived Okawa entrainment model with a modification of the film thickness calculation, which gives the best results on steam-water and air-water databases compared with other literature correlations. In the end, the final correlation for mass transfer is:

$$m_{E,Okawa} = k_E \rho_{lc} \frac{f_i \rho_g J_g^2 \delta}{\sigma} \cdot \left(\frac{\rho_{lc}}{\rho_g} \right)^{0.111} \tag{14}$$

Similarly, the deposition model is based on the diffusion of droplets in the gas core but the formula itself is slightly different than Hewitt's or Sugawara's.

$$m_{D,Okawa} = C \cdot 0.0632 \left(\frac{C}{\rho_g} \right)^{-0.5} \cdot \left(\frac{\sigma}{\rho_g D_h} \right)^{0.5} \tag{15}$$

Interesting approach is presented by Lane [24] in his PhD thesis and his publication [25]. These works attempt to “de-lump” entrainment phenomenon where the authors distinguish three different mechanisms

for entrainment (liquid bridge break-up, Kelvin-Helmholtz lifting and roll wave stripping) as well as two zones for the interfacial shear stress.
The final results were obtained with Okawa hydrodynamic model presented in Okawa [14] and compared in Adamsson and Anglart [11].

3.4 Boiling Phenomena

The model governing the evaporation of the film have a significant impact on the dryout prediction. The heat transfer involving the wall and interfacial heat transfers in CATHARE-3 is described in [3, 4]. It is assumed that the wall and interfacial heat transfer are null, that is droplets are not directly heated or cooled by the wall. The heat flux from the gas to interface of the dispersed liquid is evaluated using a convection law for flow around spheres and that from the gas to the interface of the film is modelled using a forced convection approach.
In diabatic systems, additional effects influence the mass exchange between the fields. One of such mechanisms was studies by Ueda [7]. In his study, measurements were made and correlation devised in order to predict the amount of entrainment caused by bursting of vapor. However, it should be pointed out that the experiment was performed under near atmospheric pressure and using rod geometry. This implies caution when extending its applicability to other working conditions.
Another effect that is "boiling induced" is the so-called "deposition-inhibition". Due to the vapor mass flux from the interface the droplet deposition is suppressed. Hoyer [8] proposed a model to account that effect basing on experimental data obtained in vertical round tubes at KTH for pressures varying from 1 to 10 MPa and heat flux from 300 to 1000 kW/m^2. The author claims that for high heat fluxes zero deposition rates are possible and this is consistent with assumption of Milashenko [27]. Using Ueda and Hoyer correlations in CATHARE-3, it was observed that many a time entrainment due to boiling was higher than hydrodynamic entrainment as well as high flux completely nullified the deposition processes. At the same time Milashenko presented an unusual correlation for net entrainment rate due to heat flux - accounting for both "vapour burst" and "deposition inhibition". The methodology assumes that for prevailing phenomena, the maximum of hydrodynamic and heat flux induced entrainment rate is selected. In the proposed "modelling package" for CATHARE-3 the boiling effects were disabled.

4. EXPERIMENTAL DATABASE

The entrainment and deposition phenomena are known to exist for a several decades now and there has been great effort put into understanding those. First experimental attempts to quantify these effects aimed at adiabatic equilibrium conditions where mass exchanges between droplet and liquid phases are equal and no external heating is delivered. To facilitate such conditions Hewitt and Pulling [28] at United Kingdom Atomic Energy Authority constructed a low pressure (2.4 - 4.46 bar) experimental facility. The test section was comprised of a tubular pipe 3.65 m long with inner diameter of 0.93 cm through which a constant mass flux (297 kg/(m^2.s)) of water run with changing quality. The authors reported in their publication that correlations existing at that time are unlikely to be adapted to prediction of these phenomena.
A bit different experimental measurements of high pressure (68.9 bar) were presented in Singh [29]. Apart from higher pressures (close to BWR operating conditions) higher mass fluxes (542.5 - 949.3 kg/(m^2.s)) were used.
Keeys et al. [28] performed a series of experimental runs aiming at the equilibrium conditions but contrary to his predecessors the range of mass fluxes was significantly higher (1350 - 2730 kg/(m^2.s)) which allowed him more general assessment of the aforementioned phenomena.
Wurtz [9] in his report presented measurements from over 250 experiments performed with steam-water at 30 to 90 bars under both adiabatic and diabatic conditions. The mass fluxes ranges from 500 up to 3000 kg/(m^2.s). The most noteworthy are the 200, 600 and 300 series where 1st and 2nd are focused on

analyzing the entrainment and deposition under equilibrium conditions with 1 cm and 2 cm of tube diameter respectively. The 300 series is focused on diabatic flows with 1 cm inner diameter with different heat fluxes and adiabatic lengths.

Adamsson and Anglart [11] performed another diabatic test with focus on the different heating axial profiles' influence on the film flow at the outlet. This experiment (KTH Film-flow) provided most detailed measurements as for each flow condition configuration, 7 measurement points near the outlet are given.

Table I summarizes the experimental databases used in this study.

Table I. Summary of experimental databases used in this study.

	Length [m]	D_h [cm]	Pressure [bar]	Mass flux [kg/m^{2}s]	Quality [%]	Heat flux [W/cm^2]	Runs
Hewitt-Pulling	3.65	0.93	2.39–4.46	297	14–75	–	70
Keeys	3.66	1.26	34.47–68.94	1350–2760	14–68	–	21
Singh	2.54	1.252	68.94	542–949	30–81	–	8
Wurtz 200	9	1.0	30–90	500–3000	8–60	–	72
Wurtz 600	9	2.0	70	500–3000	20–70	–	21
Diabatic tests							
KTH Film-flow	3.65	1.4	70	750–1750	40–78	100–200	21
Wurtz 300	2–6	1.0	30–90	500–3000	16–80	50–150	78

5. RESULTS

For the sake of completeness, "current version of CATHARE-3" consists of 4 models, namely: Kutateladze annular flow criterion (eq. (8)), Hewitt-Govan hydrodynamic entrainment and deposition correlations (eq. (1) and (2)), Ueda boiling entrainment (eq. (5)) and Hoyer deposition inhibition (eq. (6)). The "modified version of CATHARE-3" consists of Wallis criterion for the prediction of the onset of annular flow (eq. (11)), Okawa hydrodynamic entrainment and deposition correlations, and a new correlation for the initial fraction of entrainment (eq. (14)) and (15)).

Each new correlation for the onset of annular flow and entrainment/deposition process was tested and compared one-to-one against the corresponding current version in the experimental database. In order to separate the effects, first a comparison of entrainment/deposition correlations against the adiabatic experiments was performed. Then the criteria of the onset of annular flow were benchmarked on the diabatic tests. At least one initial fraction of entrainment was taken into account. The paper presents the results of the modified package.

For the initial fraction of entrainment (E_{init}), the initial step of the analysis was to run the KTH simulation with a fixed value equal to 0.5 in CATHARE 3 for all cases. The initial results showed that for the cases where mass flux equaled 750 kg/(m^2.s), the film flow was underpredicted, which was concluded that value of IEF was too high. For the cases of mass flux equal to 1250 kg/(m^2.s) and 1750 kg/(m^2.s) the film flow was slightly and significantly overpredicted. Having these values, it was possible to derive the following correlation, based on both KTH and Wurtz series 300:

$$E_{\text{init}} = \begin{cases} 0.3 & \text{for} \quad G < 500 \\ \dfrac{0.127 \cdot G - 60.385}{G \cdot x_{tr}} & \text{for} \quad 500 \leq G \leq 1800 \\ 0.75 & \text{for} \quad 1800 < G \end{cases} \tag{16}$$

where G is the total mass flux and x_{tr} the quality at transition to annular flow, calculated with equation (11). In accordance to Barbosa et al. [17], this correlation does not facilitate the equilibrium assumption ($m_E = m_D$). In the code, a smooth transition to Okawa's entrainment model is done downstream the onset of annular flow location. All results presented were obtained with the proposed correlation of the initial fraction entrainment.

Figure 2(a) shows the comparison of calculation of high pressure (30–90 bar) experiments. The analysis of the results has yielded that the modified package of CATHARE-3 (Okawa model) gives better results than the current version (Hewitt). Moreover, the modified version of CATHARE-3 produce significantly less spread results (approx. 3 times) than the current version.
Figure 2(b) depicts only one experiment of low pressure, namely, the Hewitt-Pulling experiment. The current model predicts results at low pressures with smaller overprediction than underprediction of modified version. Additionally, current model is characterized with much lower spread of the results. It must be pointed out that the modified package also includes the Sugawara correlation for the deposition phenomenon, for low pressures (under 5 bar) and qualities higher than 0.25, following the suggestion of Okawa which results are included Figure 2(b), however, those are not distinguished. The Sugawara correlation is only linked to the Okawa entrainment model.

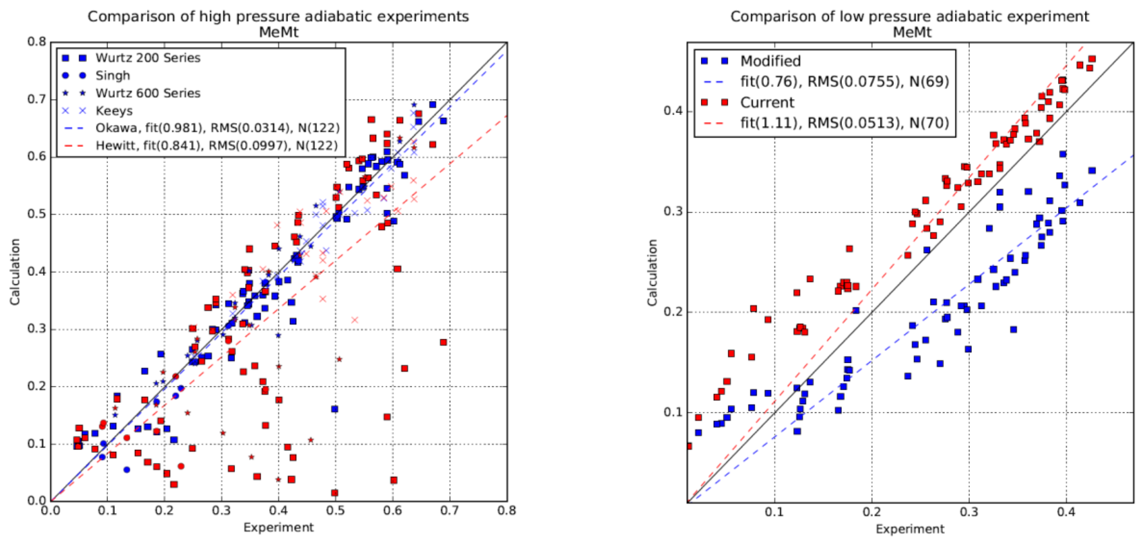

(a) **(b)**

Figure 2. (a) High pressure adiabatic tests (Singh, Keeys, Wurtz 200 series and Wurtz 600 series), (b) Low pressure adiabatic tests (Hewitt-Pulling).
Blue and red marks represent "current" and "modified" CATHARE-3"

In Figure 3a one can observe the comparison of calculation of current and modified models against experimental results obtained for the Wurtz 300 series with a heated section. Clearly, the modified version of CATHARE-3 gives better results in terms of fitting (entrained droplets are less overpredicted) and spread of results.
As far as KTH film flow experiment is concerned it was impossible to produce similar plot due to the fact that current version of CATHARE-3 severely underpredicted the CHF which resulted in dryout occurrence quite far upstream from the outlet of the test section (Figure 3b depicts results of current CATHARE-3 model in which boiling effects has been disabled.). This behavior is exemplified in Figure 4 in which the film flow versus location is plotted - blue and red lines represent the film flow for current and modified versions of CATHARE-3.

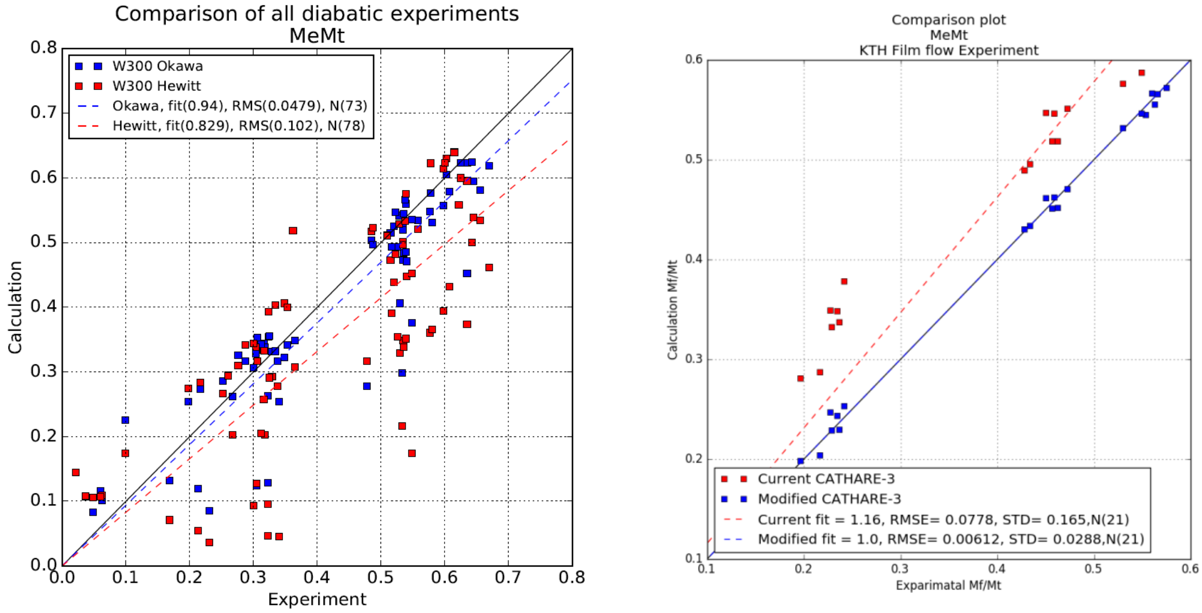

(a) (b)

Figure 3. High pressure diabatic tests: (a) Wurtz series 300, (b) KTH Film Flow

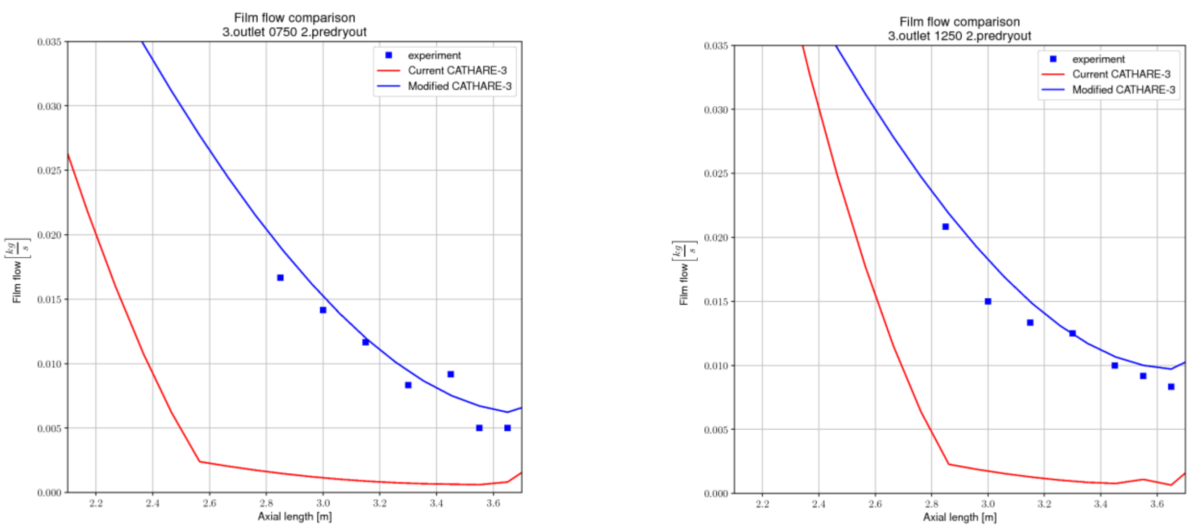

(a) (b)

Figure 4. High pressure diabatic test: KTH film flow experiment. (a) Total mass flux: 750 kg/(m²s), Heating power: 140.8 kW. (b) Total mass flux: 1250 kg/(m²s), Heating power: 166.3 kW.

5.1 Summary of Results

In Table II, calculation results are presented, in terms of M_e/M_t ratio. Film flowrate to tube perimeter ratio M_f/P has also been added in order to test a possible dependence against the tube diameter on the results. The improvements are marked with bold font. As far as M_e/M_t fitting coefficient is concerned, one can observe that in almost all cases of Okawa correlation it is in range from 0.933 to 1.03 apart from Hewitt-Pulling adiabatic test. Similar improvements are also present for the root mean square error which in

majority of cases is lower than 0.05 for the modified Okawa model. Finally, the standard deviation is three times lower in cases of Keeys and Wurtz series 600, two times lower for Singh and Wurtz series 300. Wurtz series 200 did not exhibit as significant improvement as other cases.
KTH film flow experiment showed the most improvements qualitatively and quantitatively. From the point where dryout is occurring far upstream to the point where the root mean square error is just 0.006 with really slight standard deviation.
As far as M_f/P parameter is concerned, in many cases the fitting coefficient has decreased from around 1.4 for current CATHARE-3 model to around unity for modified CATHARE-3 models. Only Wurtz series 600 (with the highest hydraulic diameter) resulted in fitting coefficient below 0.9 for modified CATHARE-3. When other parameters are compared, a noticeable increase in accuracy is observed – similarly a trifold decrease of root mean square error and standard deviation is noticed.

Table II. Comparison of the error and the standard deviation for M_e/M_t and M_f/P (in brackets) obtained on the presented database for the current and modified version of CATHARE 3.

Experiment	Fitting coefficient of M_e/M_t (M_f/P)		Root mean square error of: M_e/M_t (M_f/P)		Standard deviation of: M_e/M_t (M_f/P)	
	current	modified	current	modified	current	modified
Adiabatic						
Hewitt-Pulling	**1.11 (0.892)**	0.762 (1.07)	**0.051 (0.03)**	0.076 (0.05)	0.8 (0.13)	**0.77 (0.21)**
Keeys	0.929 (1.39)	**0.993 (1.04)**	0.078 (0.35)	**0.028 (0.1)**	0.15 (0.54)	**0.054 (0.17)**
Singh	0.698 (1.33)	**0.933 (1.02)**	0.093 (0.152)	**0.033 (0.04)**	0.4 **(0.3)**	**0.19** (0.44)
Wurtz 200	0.822 (1.49)	**0.966 (1.07)**	0.171 (0.4)	**0.057 (0.1)**	0.49 (0.6)	**0.31 (0.16)**
Wurtz 600	0.787 (1.4)	**1.030 (0.88)**	0.096 (0.34)	**0.029 (0.12)**	0.34 (0.43)	**0.11 (0.15)**
Diabatic						
KTH	–	**1.0 (0.991)**	–	**0.006 (0.025)**	–	**0.029 (0.15)**
Wurtz 300	0.829 (1.27)	**0.94 (1.01)**	0.102 (0.357)	**0.0479 (0.335)**	0.8 **(0.47)**	**0.36** (0.66)

5.2 Error Analysis

After the results were obtained an error analysis was performed. Figure 5a shows a relative error (ratio of calculated M_eM_t to measured M_eM_t) plotted against the M_f/P ratio. The highest error is exhibited for the low values of the analysed parameter – with a maximum around M_f/P=0.45, for D_h = 0.01 m only (Wurtz series 200). For Wurtz series 600, which hydraulic diameter is 0.02 m, the relative error is considerably lower. Additionally, one can see that for lowest values of film flow the calculation of the flow for 3 fields are predicting the results with 20% (and less) of accuracy (with an exception of one Singh case).
Similar plot is achieved for vapour mass flux (Figure 5b). In this case there is a noticeable break-point where the error is the highest, namely for value of 300 kg/(m^{2}s). Extensive analysis of model performance in different regions of flow conditions would be highly interesting.

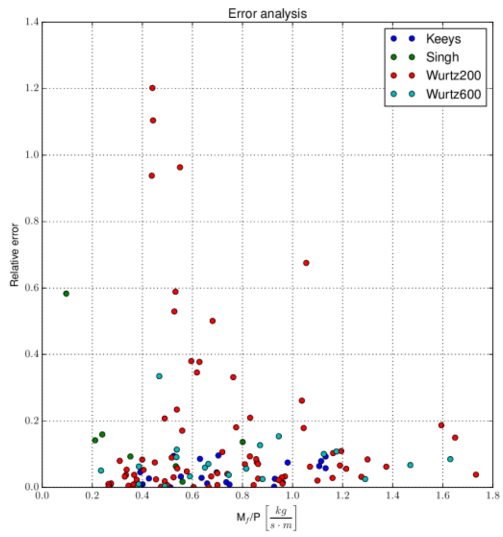

(a)

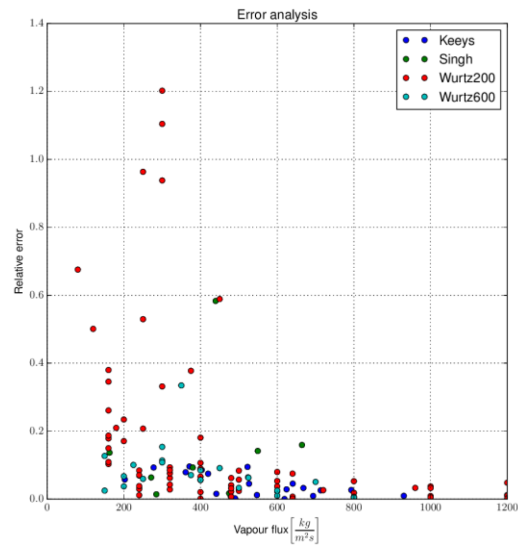

(b)

Figure 5. Spectrum of relative error with respect to (a) M_f/P and (b) Vapour mass flux (kg/m^{2}s) for four high pressure adiabatic experiments.

6. CONCLUSIONS AND PERSPECTIVES

With all the available data acquired during this work it is clear that "modified" Okawa modeling package is superior to the Hewitt-Govan default set of models within CATHARE-3 in high pressure conditions. Adiabatic experiments showed that Okawa correlation provides results with higher accuracy and lower standard deviation when compared to the current model of CATHARE-3 code. Also, error analysis identified weak and strong points of the entrainment and deposition correlation which should be addressed in future.

Moreover, it was proved that models for entrainment due to boiling and deposition inhibition do not improve the acquired solution in high heat flux conditions and at the same time do not play important role during low heat flux operating conditions. This observation can be explained in twofold. Firstly, albeit these effects may occur in reality they were measured in low pressure condition and quantitatively these effects are not approximated well enough for high pressure conditions. Secondly, the correlations describing the entrainment and deposition have been approximated on some diabatic data and hence these effects could be partly lumped in the existing correlations. Separation and measurement of these effect is still a challenging feat.

The role of Initial Entrainment Fraction was also shown to be crucial in proper estimation of film flows and thus dryout power. The rough IEF correlation still requires more work in order to develop more mechanistic model validated on broader set of conditions. Sensitivity analysis of the proposed correlation is also required.

NOMENCLATURE

C	- Concentration of droplets, [kg/m^3]	k	- coefficient
D_h	- hydraulic diameter, [m]	k_q	- deposition inhibition due to boiling effects,
E	- Entrained Fraction, [-]	Ku	- Kutateladze number, [-]
f	- friction factor	m	- mass flow per wetted area, [kg/(m^{2}s)]

g	- gravity acceleration [m/s^2]	MeMt	- entrained droplet to total mass flow ratio [-]
G	- mass flux, [kg/m^2/s]	P	- tube perimeter, [m]
G_{lfc}	- critical film mass flux, [kg/(m^{2}s)]	q''	- Heat flux, [W/m^2]
h_{fg}	- latent heat of evaporation, [J/kg]	V	- Velocity, [m/s]
J	- Superficial velocity, [m/s]	x	- flow quality
J^*	- dimensionless superficial velocity, [m/s]		

Greek

α	- void fraction, [-]	μ	- dynamic viscosity, [kg/(m.s)]
δ	- film thickness, [m]	π_E	- dimensionless number
Γ	- evaporation rate [kg/m^{2}s]	ρ	- density [kg/m^3]
		σ	- surface tension[N/m]

Subscript

B	- Boiling related	i	- interface
d	- droplet related	init	- initial
D	- Deposition	HG	- Hewitt-Govan
E	- Entrainment	l	- liquid related
eq	- equilibrium related	v	- vapour related
f	- film related	tr	- transition to annular flow

ACKNOWLEDGMENTS

This collaboration work between CEA (Commissariat à l'Énergie Atomique et Aux Énergies Alternatives, France) and NCBJ (National Centre for Nuclear Research, Poland) has been achieved in the framework of the NEPTUNE project, financially supported by CEA, EDF, IRSN (Institut de Radioprotection et de Sûreté Nucléaire) and AREVA-NP. This work has also been financially supported by the International Relations Division of CEA.

REFERENCES

1. G.F. Hewitt and N.S. Hall-Taylor, *Annular Two-phase Flow*, Pergamon (1970).
2. P.B. Whalley, P. Hutchinson, and G.F. Hewitt. "The calculation of critical heat flux in forced convective boiling", *Proceedings of the 5th International Heat Transfer Conference,* Tokyo, Japan, (1974).
3. S. Jayanti and M. Valette, "Prediction of dryout and post-dryout heat transfer at high pressures using a one-dimensional three-fluid model", *International Journal of Heat and Mass Transfer*, **47**, pp. 4895–4910 (2004).
4. S. Jayanti and M. Valette, "Calculation of dry out and post-dry out heat transfer in rod bundles using a three field model", *International Journal of Heat and Mass Transfer*, **48**, pp. 1825–1839 (2005).
5. M. Valette, J. Pouvreau, D. Bestion and P. Emonot, "Revisiting large break LOCA with the CATHARE-3 three-field model", *Nuclear Engineering and Design*, **241**, pp. 4487–4496 (2011).
6. G.F. Hewitt and A.H. Govan, "Phenomenological modelling of non-equilibrium flows with phase change", *International Journal of Heat and Mass Transfer*, **33**(2) pp. 229–242 (1990).
7. T. Ueda, M. Inoue, and S. Nagatome, "Critical heat flux and droplet entrainment rate in boiling of falling liquid films", *International Journal of Heat and Mass Transfer,* **24**(7) pp. 1257-1266 (1981).
8. N. Hoyer, "Calculation of dryout and post-dryout heat transfer for tube geometry", *International Journal of Multiphase Flow*, 24(2) pp. 319–334 (1998).

9. J. Wurtz, “An experimental and theoretical investigation of annular steam-water flow in tubes and annuli at 30 to 90 bar”, Technical Report no 372, Risø National Laboratory, Denmark (1978).
10. T. Okawa, T. Kitahara, K. Yoshida, T. Matsumoto, and I. Kataoka, “New entrainment rate correlation in annular two-phase flow applicable to wide range of flow condition”, *International Journal of Heat and Mass Transfer*, **45**(1) pp. 87-98 (2002).
11. C. Adamsson and H. Anglart, “Film flow measurements for high-pressure diabatic annular flow in tubes with various axial power distributions”, *Nuclear Engineering and Design*, **236** pp. 2485-2493 (2006).
12. S. Kutateladze, “Elements of the Hydrodynamics of Gas-Liquid Systems”, Fluid Mechanics-Soviet Research, Tech. Rep. AERE-R6293 (1972).
13. G.B. Wallis. *One-Dimensional Two-Phase Flow*. McGraw-Hill (1969).
14. T. Okawa, A. Kotani, I. Kataoka, and M. Naito, “Prediction of Critical Heat Flux in Annular Flow Using a Film Flow Model”, *Journal of Nuclear Science and Technology*, **40**(6) pp. 388-396 (2003).
15. S. Sugawara, “Droplet deposition and entrainment modeling based on the three-fluid model”, *Nuclear Engineering and Design*, **122**(1-3) pp. 67-84 (1990).
16. A. H. Govan, *Modelling of vertical annular and dispersed two-phase flows*. PhD thesis, Imperial College, University of London, 1990.
17. J.R. Barbosa Jr., G.F. Hewitt, G. Konig, and S.M. Richardson, “Liquid entrainment, droplet concentration and pressure gradient at the onset of annular flow in a vertical pipe”, International Journal of Multiphase Flow, **28**(6) pp. 943-961 (2002).
18. H. Anglart, “Investigation of local dryout conditions in forced convection to water at high pressure in uniformly and non-uniformly heated vertical round tubes and annuli”, *Proceedings of NURETH-15*, Pisa, Italy (2013).
19. S. Oh, B. Hizoum, P. Saha, B. Dooies, and D. Miranda, “Film-droplet split correlation at the onset of annular-mist flow”, *Proceedings of NURETH-15*, Chicago, USA (2015).
20. A. Dasgupta, D.K. Chandraker, A.K. Vishnoi, and P.K. Vijayan, “A new methodology for estimation of initial entrainment fraction in annular flow for improved dryout prediction”, Annals of Nuclear Energy **75** pp. 323-330 (2015).
21. A. Dasgupta, D.K. Chandraker, and P.K. Vijayan, “SCADOP: Phenomenological modeling of dryout in nuclear fuel rod bundles”, *Nuclear Engineering and Design*, **293** pp. 127-137 (2015).
22. T. Okawa, A. Kotani, I. Kataoka, and M. Naito, “Prediction of the critical heat flux in annular regime in various vertical channels”, *Nuclear Engineering and Design*, **229** pp. 223-236 (2004).
23. T. Okawa and I. Kataoka, “Correlations for the mass transfer rate of droplets in vertical upward annular flow”, *International Journal of Heat and Mass Transfer*, **48**(23-24) pp. 4766-4778 (2005).
24. J. W. Lane. “The development of a comprehensive annular flow modeling package for two-phase three-field transient safety analysis codes”, PhD thesis, The Pennsylvania State University, (2009).
25. J. W. Lane, D. L. Aumiller, F.-B. Cheung, and L. E. Hochreiter, “A self-consistent three-field constitutive model set for predicting co-current annular flow”, *Nuclear Engineering and Design*, **240** pp. 3294–3308 (2010).
26. F. Secondi, C. Adamsson and J.-M. Le Corre, “An assessment of entrainment correlations for the dryout prediction in BWR fuel bundles”, *Proceeding of NURETH-13*, Kanazawa, Japan (2009).
27. V. I. Milashenko, B. I. Nigmatulin, V. V. Petukhov, and N. I. Trubkin, “Burnout and distribution of liquid in evaporative channels of various lengths”, *International Journal of Multiphase Flow*, **15** pp. 393-402 (1989).
28. G. F. Hewitt and D. J. Pulling, “Liquid entrainment in adiabatic steam-water flow”, Technical Report AERE-R5374, UKAEA (1969).
29. K. Singh, C. C. St. Pierre, W. A. Cargo, and E. O. Moeck, “Liquid film flow rates in two-phase flow of steam and water at 1000 psia”, AIChE Journal, **15** pp. 51-56 (1969).
30. R. K. F. Keeys, J. C. Ralph, and D. N. Roberts, “Liquid entrainment in adiabatic steam-water flows at 500 and 1000 P.S.I.A (3.447 and 6.894×10^6 N/m^2)”, Technical Report AERE-R6293, UKAEA (1970).